Mixed Cation Zeolites: $Li_x Ag_y$-X as a Superior Adsorbent for Air Separation

Nick D. Hutson, Salil U. Rege, and Ralph T. Yang
Dept. of Chemical Engineering, University of Michigan, Ann Arbor, MI 48109

Li-X zeolite (Si/Al = 1.0) is currently the best sorbent for use in the separation of air by adsorption processes. Silver is also known to strongly affect the adsorptive properties of zeolites and thermal vacuum dehydration of silver zeolites leads to the formation of silver clusters within the zeolite. In this work we synthesized type X zeolites containing varying mixtures of Li and Ag. Adding very small amounts of Ag at the proper dehydration conditions formed silver clusters and enhanced adsorptive characteristics and energetic heterogeneity, as compared to those of the near fully exchanged Li^+-zeolites. The performance for air separation by the best of these sorbents, containing, on average, only one Ag per unit cell, was compared to that of the near fully Li^+-exchanged zeolite using a standard PSA cycle by numerical simulation. The results show that the new sorbent provides a significantly higher (> 10%) product throughput at the same product purity and recovery when compared to that of the near fully Li^+-exchanged zeolite.

Introduction

The separation of air for the production of nitrogen and oxygen is a very important operation in the chemical processing industries. Historically, this separation has been done predominately by cryogenic distillation; though, as adsorption systems have become more efficient and new, more effective sorbents have been synthesized, separation by adsorption processes (such as pressure swing adsorption (PSA) and vacuum swing adsorption (VSA)) have become increasingly competitive and are already favorable for small-to-medium scale operations (Yang, 1997a). Currently, approximately 20% of air separations are accomplished using adsorption technologies (Rege and Yang, 1997).

Since their introduction in the 1950s, synthetic zeolites have been used in numerous applications such as catalysis, ion exchange, drying, and separation by selective adsorption. In the separation of air, zeolites of type A and X have typically been used. The A and X type zeolites are composed of silica and alumina tetrahedra, which are joined together to form the truncated octahedral or sodalite structure. These sodalite units are connected with tertiary units to form the structured zeolite unit cell. While the SiO_2 groups are electroneutral, the $(AlO_2)^-$ groups are not, and thus introduce a negative charge to the structure which is offset by the presence of a charge compensating, nonframework cation (such as Na^+, Li^+, Ca^{2+}). Type X zeolites contain between 77 and 96 Al per unit cell. The unit cell, including cation sites, for type X zeolite is shown in Figure 1.

It is known that the extra-framework cations in the zeolite are largely responsible for the nitrogen selectivity of these

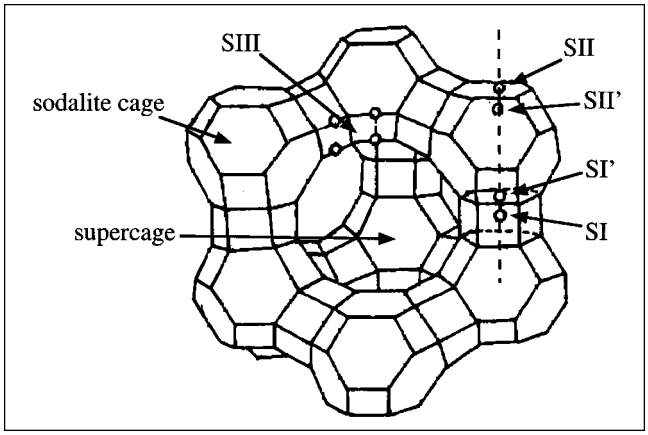

Figure 1. Unit cell of faujasite-type (X and Y) zeolites including cation sites.

Correspondence concerning this article should be addressed to R. T. Yang.

materials (Barrer, 1978; Breck, 1984). These zeolites adsorb nitrogen preferentially to oxygen (usually at a ratio of about 4:1) due primarily to the interaction between the charge compensating cations of the zeolite and the quadrupole moment of the adsorbing gas (N_2 or O_2). The quadrupole moment of N_2 is approximately four times that of O_2. Because the extra-framework cations so significantly influence the adsorption properties of the zeolites, numerous attempts have been made to optimize these properties by: (1) increasing the number of cation sites (the cation exchange capacity or CEC) by creating zeolites with high aluminum content; (2) by synthesizing zeolites containing various combinations of alkaline and alkaline earth cations.

Kuhl (1987) reported a procedure for the synthesis of low silica X-type zeolite (LSX). This material is an aluminum saturated X-type zeolite with a silica-to-alumina ratio of 2.0 (or Si/Al = 1.0). Commercial X-zeolite, which is typically available as the Na^+ form (known commercially as 13X), is not aluminum saturated and contains 86 aluminum atoms per unit cell, while the low silica X zeolite contains 96 aluminum atoms per unit cell.

While it has long been known that Li^+ is among the strongest cations, with respect to its interaction with N_2 (McKee, 1964), its use was greatly increased with two recent advances. First, it was found that Li^+ ion-exchange in X-type zeolite must exceed an approximate 70% threshold before the Li^+ has any effect on the adsorptive properties of the material (Chao, 1989; Chao et al., 1992; Coe et al., 1992, 1995). Secondly, a significant increase in the N_2 adsorption capacity was seen in the Li^+ ion-exchanged low silica X-type zeolites over that of the typical commercial material (Si/Al = 1.25). Because of these advances, Li-X (Si/Al = 1.0) is now the best sorbent in industrial use for separation of air by adsorption processes (Yang, 1997b; Rege and Yang, 1997).

Coe et al. (1992) reported the use of a binary exchanged X-zeolite having lithium and calcium and/or lithium and strontium ions in a ratio of 5% to 50% calcium and/or strontium and 50% to 95% lithium. This material provided for enhanced nitrogen adsorption over those of the Na-X, Li-X, and Ca-X zeolites. Chao et al. (1992) reported the use of mixed ion-exchanged A and X zeolites with lithium and an alkaline earth metal (such as Ca^{2+}, Sr^{2+}). In this case the zeolite contained lithium and the alkaline earth cations in a mixture of 10% to 70% alkaline earth and 30% to 90% lithium. These mixed cation zeolites provided high adsorption capacity and high thermal stability. Fitch et al. (1995) reported good N_2/O_2 selectivity and N_2 capacity with mixed Li_xAl_y-X zeolite (that is, using Ag^{3+} as the nonframework charge-compensating cation).

Silver is also known to have very strong effects on the adsorption characteristics of zeolites (Habgood, 1964; Huang, 1974). Yang et al. (1996) reported the synthesis of a mixed lithium-silver (80/20) ion-exchanged X-type zeolite (Si/Al = 1.25) with approximately 17 Ag^+ per unit cell), and discussed its possible superior properties for air separation. This sorbent utilized the very strong adsorptive properties of the Ag^+ ion which provided for increased capacity over that of the Li-X while maintaining some degree of the advantageous isotherm linearity that is seen with Li-X. *Ab initio* molecular orbital calculations showed the adsorption of nitrogen was enhanced by weak chemical interaction (through a classical π-complexation bond) with the Ag^+ cation on the zeolite framework (Chen and Yang, 1996).

Numerous attempts have been made to reduce transition metal ions in zeolites for the purpose of forming highly dispersed metallic clusters for use as catalysts. These attempts have typically been completed via treatment at elevated temperatures and/or in reducing atmospheres (such as sodium vapor, hydrogen gas, carbon monoxide gas). However, color changes upon vacuum dehydration of silver-exchanged A-type zeolites were found to be related to the formation of metallic clusters within the sodalite cage or the 6-prism of the zeolite (Kim and Seff, 1978a,b; Jacobs et al., 1979). Using volumetric sorption techniques and temperature programmed desorption, Jacobs et al. (1979) were able to relate these color changes to an autoreductive process involving framework oxygen.

Autoreduction is the reduction of the transition metal ion and the oxidation of water or lattice oxygen; this has been observed for both Ag^+ and Cu^{2+} ions in zeolites A, X and Y, and has been shown to take place by two mechanisms in two clearly defined temperature regions (Jacobs et al., 1979; Baker et al., 1985)

(i) autoreduction in the presence of zeolite water (25–250°C)

$$2(Ag^+\text{-Z-}O^-) + H_2O \rightarrow 2Ag^0 + (1/2)O_2 + 2\text{Z-OH} \quad (1)$$

and (ii) autoreduction by oxygen from the zeolite lattice (127–380°C)

$$2(Ag^+\text{-Z-}O^-) \rightarrow 2Ag^0 + (1/2)O_2 + \text{Z-}O^- + Z^+ \quad (2)$$

Kim and Seff (1978a,b) proposed the formation of octahedral hexasilver metal clusters stabilized by coordination to six silver ions ($(Ag^+)_6(Ag)^6$) from x-ray structural determinations of a dehydrated silver-exchanged zeolite A. However, Jacobs et al. (1979) suggested that the formation of such large metal clusters is improbable since color changes are seen even at low temperatures and low silver loadings where extensive migration of neutral silver atoms and subsequent sintering into Ag_6 metal clusters is highly unlikely. Alternatively, Jacobs et al. (1979) suggested, based on structural studies of Ag-A zeolites, the formation of linear $(Ag_3)^{2+}$ charged clusters (Ag^+-Ag^0-Ag^+) upon thermal dehydration of the zeolite.

Gellens et al. (1981a,b, 1983) followed color changes and concomitant silver cluster formation in A, X, and Y zeolites using X-ray diffraction (XRD) techniques. They found that the number of clusters increases with framework Al content. It was also noted that in synthetic analogs of the faujasite zeolite (types X and Y) the dehydrated zeolites displayed a yellow color which increased in intensity with the number of clusters, while silver-exchanged A zeolites took a yellow color with dehydration at low temperatures, eventually becoming brick red after treatment at higher temperatures.

In this work we have synthesized type X zeolites containing varying amounts of Li and Ag. We have treated these materials in a way which promotes the formation of intracrystalline silver clusters, and we have evaluated the resulting adsorptive

characteristics with respect to the gases which are of primary interest in the separation of air: N_2, O_2, and Ar. The performance of the best of these materials was compared to that of the fully Li^+-exchanged zeolite using a numerical simulation of a standard five-step PSA cycle (that is used in industry). The results are given below. A broader range of mixed-cation zeolites as well as their applications are given elsewhere (Yang and Hutson, 1998).

Experimental Studies

Materials

Two type-X zeolites, differing only by the Si/Al ratio, were used in this work. These were: (1) X-type zeolite with a Si/Al of 1.0 (Praxair, No. 16193-42, sometimes referred to as LSX, low silica X-zeolite); (2) X-type zeolite with a Si/Al of 1.25 (Linde, lot 945084060002). Both of these materials were binderless, hydrated powders.

Helium (99.995%, prepurified), oxygen (99.6%, extra dry), nitrogen (99.998%, prepurified), and argon (99.998% prepurified) were obtained from Cryogenic Gases. All water used was deionized.

Cation exchange

Since the sodium form of the zeolite exchanges more readily with most cations in consideration, all zeolites were first ion exchanged with a solution of sodium chloride in order to convert to the Na^+ form. A dilute NaOH solution was used to keep the NaCl solution at pH $\approx$ 9. This helps to prevent hydrolysis and breakdown of the zeolite crystal structure during the ion-exchange process. The resultant Na^+-zeolite was then used as the starting material for all other syntheses.

Preparation of Li-zeolites

The lithium zeolites were prepared by five consecutive static ion exchanges using a 6.3-fold excess (over that necessary for full ion exchange) of a 2.2 M solution of LiCl. This was done in a 0.01 M solution of LiOH at a pH $\approx$ 9. The lithium ion-exchange solution was heated to a mild boil and then allowed to cool and settle. The solution was decanted, a fresh 6.3X LiCl solution was added, and the procedure was repeated for a total of five exchanges. After the final ion exchange, the material was vacuum filtered and washed with copious amounts of deionized water until no free ions were present in the filter water (that is, no precipitation upon treatment with Ag^+). The resulting lithium exchanged zeolites were dried overnight at 100°C in a conventional oven before being dehydrated *in vacuo* prior to measurement of adsorption isotherms.

Preparation of Ag-zeolites

The silver zeolites were prepared by two consecutive ion exchanges using a 0.05 M solution of $AgNO_3$. Each silver solution contained a cation content which was double that required for 100% exchange. The silver ion-exchange solution was heated to a mild boil and immediately allowed to cool and settle. As with the lithium ion exchange, the solution was decanted, fresh $AgNO_3$ solution was added, and the procedure was repeated for a total of two exchanges. After the second ion exchange, the material was vacuum filtered and washed with copious amounts of deionized water until no free ions were present in the filter water (no precipitation upon treatment with Cl^-). The silver exchanged materials were dried at room temperature and atmospheric conditions in a dark area. The resulting materials were then stored in a dark area until they were dehydrated *in vacuo* prior to analysis.

Preparation of Li_xAg_y-zeolites

The Li_xAg_y-zeolites (which may more accurately be referred to as $Li_xNa_yAg_z$-zeolites since ion exchange is rarely exhaustive and there is almost always some residual Na^+ present in the starting Li-zeolite) were prepared by ion exchange of a Li-zeolite (prepared as described above) with a 0.05 M solution of $AgNO_3$. This silver solution contained a cation content which was equivalent to the targeted amount. This is possible with silver ion exchange, because the silver cation is quickly and easily exchanged (Breck, 1984). The silver ion-exchange solution was heated to a mild boil and immediately allowed to cool and settle. The resulting material was vacuum filtered and washed with copious amounts of deionized water. Complete incorporation of the targeted silver ions was verified when no precipitation was observed in the filtered water on treatment with Cl^-. These mixed cation zeolites were then dried at room temperature and atmospheric conditions in a dark area and were stored in a dark area until they were dehydrated *in vacuo* prior to analysis.

Dehydration

Prior to measurement of the adsorption isotherms or uptake rates, it is necessary to dehydrate the zeolite sample. Zeolites have a strong affinity for water, and some molecules are tenaciously held. The presence of water in the zeolite significantly affects the validity of the adsorption measurement. Prior to analysis, all samples were heated in order to remove water. Differential thermal analysis (DTA) of zeolite X has shown a continuous loss of water over a broad range of temperatures, starting at slightly above room temperature up to 350°C with a maximum at about 250°C (Breck, 1984). Specific dehydration conditions varied and are given for each sample.

Characterization

The samples were compositionally characterized using neutron activation analysis (NAA) in the research nuclear reactor of the Phoenix Memorial Laboratory at the University of Michigan. The samples were irradiated sequentially for one minute at a core-face location with an average thermal neutron flux of 2×10^{12} n/cm^2/s. Two separate gamma-ray spectra were then collected for each sample with a high resolution germanium detector: one after a 13 min decay to determine the concentrations of Al and Ag, and a second after a 1 h and 56 min decay to analyze for Na and K; both were for 500 s real time. Four replicates of NBS-SRM-1633a (coal fly ash) and silver foil were used as standard reference materials and check standards.

Table 1. Elemental Composition of Li_xAg_y-X-1.0 Zeolite Samples*

	Sample 1		Sample 2		Sample 3		Sample 4		Sample 5		Sample 6	
Comp.	wt. %	+/−	wt. %	+/−	wt. %	+/−	wt. %	+/−	wt. %	+/−	wt. %	+/−
Al	21.38	0.88	21.19	0.87	20.80	0.85	19.45	0.81	18.37	0.75	11.91	0.49
Ag	0.00	—	0.93	0.06	3.04	0.06	9.57	0.16	15.64	0.12	55.49	0.27
Na	0.28	0.02	0.14	0.01	0.10	0.01	0.11	0.01	0.22	0.01	0.03	0.01
Li	5.59	—	5.21	—	4.99	—	4.76	—	3.85	—	0.00	—

*Lithium was measured by inductively coupled plasma-mass spectroscopy (ICP-MS); all others were measured by neutron activation analysis (NAA).

The samples were also analyzed for Li content using an inductively coupled plasma mass spectrometer (ICP-MS, Hewlett Packard HP 4500). The samples were first digested in concentrated nitric acid solution at 100°C for 20 min. At the end of digestion, the samples were further diluted and filtered before the ICP-MS analyses.

The adsorption isotherms were measured using a static volumetric system (Micromeritics ASAP-2010). Additions of the analysis gas were made at volumes required to achieve a targeted set of pressures. A minimum equilibrium interval of 9 s with a tolerance of 5% of the target pressure (or 0.007 atm, whichever is smaller) was used to determine equilibrium for each measurement point. The pressure transducers in the ASAP-2010 are accurate to $< 0.2\%$ for the pressure range of 0−1 atm. The sample weights were obtained using a digital laboratory balance which is accurate to ± 0.01 g. The isotherm measurements and the samples themselves were found to be highly reproducible.

Results and Discussion

All samples are identified according to the type of zeolite, the number of charge compensating cation(s) present in a unit cell, and the Si/Al ratio. For example, Li_{86}-X-1.25 refers to an X-type zeolite with Si/Al = 1.25 which has been fully exchanged to contain 86 Li^+ cations per unit cell. The sample $Li_{94.2}Na_{0.7}Ag_{1.1}$-X-1.0 refers to an X-type zeolite with Si/Al = 1.0 which contains, on average, 94.2 Li^+, 0.7 Na^+, and 1.1 Ag^+ (or other forms of Ag) per unit cell, as determined from the neutron activation (NA) and ICP-MS analyses.

Analytical characterization

As mentioned earlier, the samples were compositionally characterized using neutron activation analysis (NAA) and inductively coupled plasma mass spectroscopy (ICP-MS). Results of these analyses are given in Table 1. The unit cell compositions for those analyzed samples are given in Table 2.

Table 2. Unit Cell Composition for Each of the Li_xAg_y-X-1.0 Samples

	1	2	3	4	5	6
Comp.	atm/uc	atm/uc	atm/uc	atm/uc	atm/uc	atm/uc
Al	96.0	96.0	96.0	96.0	96.0	96.0
Ag	0.0	1.1	3.5	11.5	21.0	95.7
Na	1.5	0.7	0.5	0.6	1.2	0.3
Si	96.0	96.0	96.0	96.0	96.0	96.0
Li	94.5	94.2	92.0	83.9	73.8	0.0
O	384.0	384.0	384.0	384.0	384.0	384.0

Adsorption isotherms for fully exchanged Li and Ag zeolites

Figure 2 shows the N_2, O_2 and Ar adsorption isotherms, measured at 25°C, for $Li_{94.5}Na_{1.5}$-X-1.0 after vacuum dehydration at 350°C. This zeolite is used in adsorptive air separation because of its very high N_2 capacity and very favorable N_2:O_2 selectivity (approximately 6:1 at 1 atm), as well as its N_2 isotherm linearity. Figure 3 shows the enchancement in the N_2 adsorptive capacity for $Li_{94.5}Na_{1.5}$-X-1.0 over that of $Li_{77}Na_9$-X-1.25.

Figure 4 shows N_2, O_2 and Ar adsorption isotherms for $Ag_{95.7}Na_{0.3}$-X-1.0, all measured at 25°C, after vacuum dehydration at 450°C for a minimum of 4 h. These samples were all initially gray in color, but, after vacuum dehydration, turned to a deep golden yellow, indicating the formation of silver clusters. Figure 5 shows the enhancement in the N_2 adsorption capacity for $Ag_{95.7}Na_{0.3}$-X-1.0 over that of the $Ag_{85.7}Na_{0.3}$-X-1.25. While the near fully exchanged Ag-zeolites, like their Li-zeolite analogs, have very high N_2 capacity and favorable N_2:O_2 selectivity, they are not favorable for use in adsorption-based separations. Because of the strong adsorption of N_2 at low pressure, creating a low-pressure "knee" in the adsorption isotherm shown in Figure 4, the working capacity (that is, the ΔQ, the change in the adsorptive capacity from the typically used adsorption pressure of 1.0 to a desorptive pressure of 0.33 atm) is very small, and the material must be exposed to very low-pressure conditions in order to increase that working capacity.

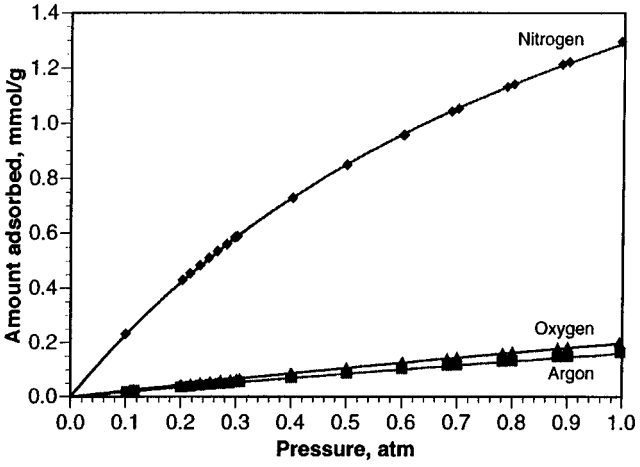

Figure 2. Adsorption isotherms for N_2, O_2 and Ar measured at 25°C for $Li_{94.5}Na_{1.5}$-X-1.0 dehydrated *in vacuo* at 350°C.

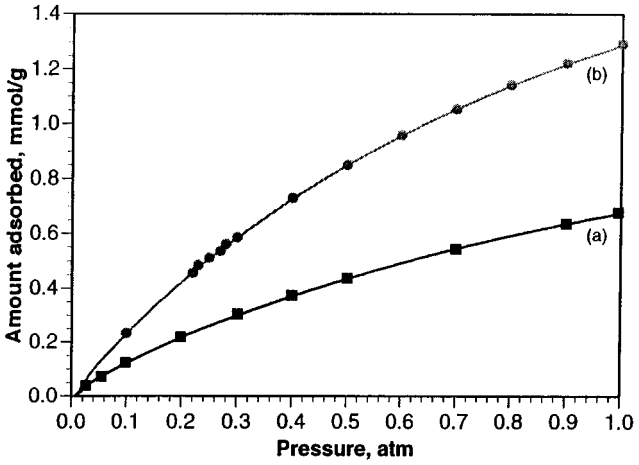

Figure 3. N_2 adsorption isotherms, measured at 25°C, for (a) $Li_{77}Na_9$-X-1.25 and (b) $Li_{94.5}Na_{1.5}$-X-1.0.

Both materials were dehydrated *in vacuo* at 350°C.

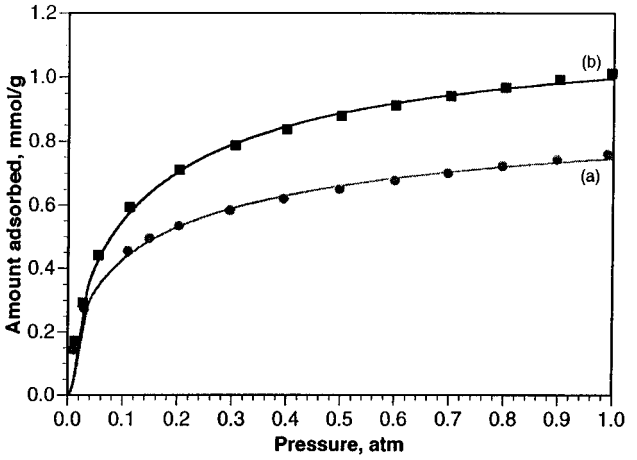

Figure 5. N_2 adsorption isotherms, measured at 25°C, for (a) $Ag_{85.7}Na_{0.3}$-X-1.25 and (b) $Ag_{95.7}Na_{0.3}$-X-1.0.

Both materials were dehydrated *in vacuo* at 450°C.

Some Ag-zeolites have been shown to have a selectivity for Ar over O_2 (Knaebel and Kandybin, 1993), and, in our work, the Ag-zeolites which had been dehydrated *in vacuo* at 350°C also showed a selectivity for Ar over O_2. However, the Ag-zeolites which had been dehydrated *in vacuo* at 450°C had approximately the same adsorption capacity for Ar and O_2 (as shown in Figure 4). This is probably due to increased interaction between the charged Ag-clusters and the quadrupole moment of the O_2 molecule (whereas, the Ar has no quadrupole moment).

Adsorption isotherms for mixed cation (Li_xAg_y) zeolites

The N_2 adsorption isotherms, measured at 25°C, for Li_xAg_y-X-1.0 zeolites after vacuum dehydration at 450°C for a minimum of 4 h are shown in Figure 6. These zeolites contained varying amounts of Ag per unit cell ranging from zero (that is, the near fully exchanged $Li_{94.5}Na_{1.5}$-X-1.0 sample) to 21 (the $Li_{73.8}Na_{1.2}Ag_{21}$-X-1.0 sample). This plot reveals that the incorporation of only a small amount of silver changes the adsorptive properties of the near fully exchanged $Li_{94.5}Na_{1.5}$-X-1.0 zeolite. With increasing additions of Ag^+ (and corresponding removal of Li^+ and Na^+), the adsorption isotherms begin to take on more of the characteristics of the near fully exchanged $Ag_{95.3}Na_{0.3}$-X-1.0 material (that is, the high ''knee'' at low pressures).

Dehydration and formation of Ag-clusters

As mentioned earlier, zeolites have a strong affinity for water, and some molecules are held tenaciously. The materials

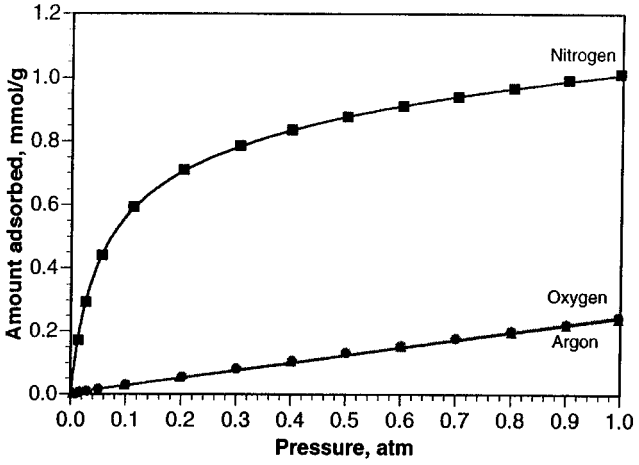

Figure 4. Adsorption isotherms measured at 25°C for N_2, O_2 and Ar on $Ag_{95.7}Na_{0.3}$-X-1.0 dehydrated *in vacuo* at 450°C.

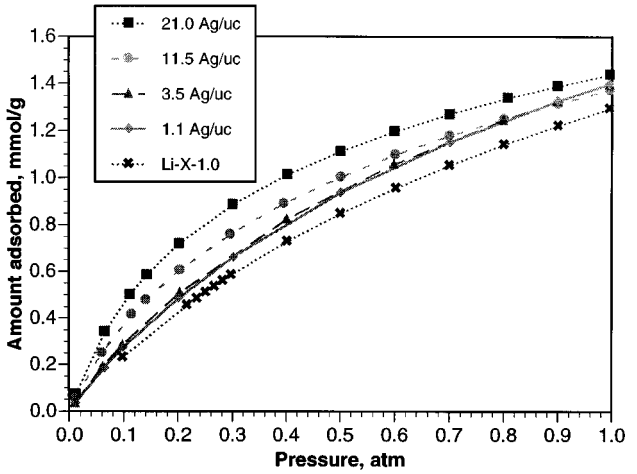

Figure 6. N_2 adsorption isotherm, measured at 25°C, for Li_xAg_y-X-1.0 zeolites dehydrated *in vacuo* at 450°C.

This shows that the addition of increasing amounts of Ag results in a change in the general aspect of isotherm toward that of the near fully Ag^+-exchanged material.

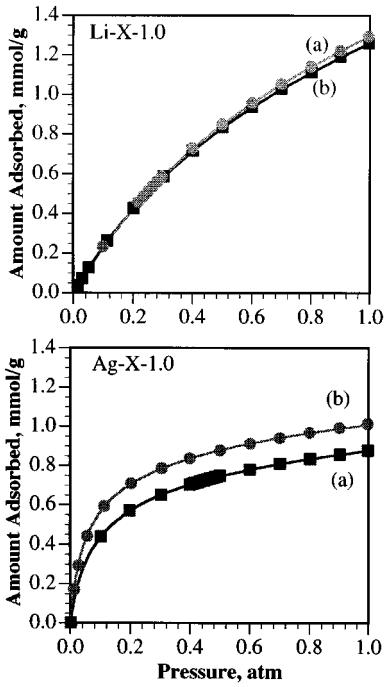

Figure 7. N_2 adsorption isotherm, measured at 25°C, for $Li_{94.5}Na_{1.5}$-X-1.0 (top) and $Ag_{95.7}Na_{0.3}$-X-1.0 (bottom).

Materials were dehydrated *in vacuo* at (a) 350°C and (b) 450°C.

must be completely dehydrated prior to measurement of the adsorption isotherms to guarantee the validity of the result. Further, the dehydration conditions have a significant effect on the formation silver clusters (Kim and Seff, 1978a,b; Gellens et al., 1981a,b) with the atmosphere and temperature of the dehydration being the most important. Figure 7 shows N_2 adsorption isotherms for $Li_{94.5}Na_{1.5}$-X-1.0 (top) and $Ag_{95.7}Na_{0.3}$-X-1.0 (bottom), both after vacuum dehydration at 350°C and 450°C. For the near fully exchanged Li material, there is no significant increase in the N_2 capacity (or in the shape of the adsorption isotherm) for the material dehydrated at 450°C over that dehydrated at 350°C. This is expected as the majority of zeolitic water is easily removed by 250°C, and most tenaciously held water molecules are removed by 350°C (Breck, 1984). However, the near fully exchanged $Ag_{95.7}Na_{0.3}$-X-1.0 sample does show an increase in N_2 capacity after dehydration at 450°c over that of the same sample dehydrated at 350°C. This increase cannot be attributed a loss of water since all but the most tenaciously held water is removed by 350°C, and there is no increase in the N_2 capacity for other zeolite forms (Li^+, Na^+, K^+, and so on) with dehydration at temperatures beyond 350°C. This increase, therefore, was the result of the formation of charged silver clusters in the zeolite with dehydration at high temperature.

A series of N_2 adsorption isotherms was measured for $Ag_{95.7}Na_{0.3}$-X-1.0 and $Li_{73.8}Na_{1.2}Ag_{21}$-X-1.0 after partial or full dehydration in vacuum at various temperatures. The results for both zeolites showed a continual increase in the N_2 adsorption capacity (at 1 atm) with increasing dehydration temperature up to 450−500°C. Materials which had been dehydrated in vacuum at 550°C and 600°C had N_2 capacities which were considerably lower than those dehydrated in vacuum at 450−500°C.

It is obvious that the ultimate adsorptive characteristics of the silver-containing zeolites are very dependent upon the formation of silver clusters and, therefore, on the dehydration conditions. We have found that best results are given when the silver-containing zeolites are dried at room temperature before being completely dehydrated in vacuum at a temperature of at least 450°C, but no greater than 500°C. The zeolites should be held at the dehydration temperature for a minimum of 4 h.

Heat of adsorption and energetic heterogeneity

Heterogeneity in zeolites may result from a number of causes including a mixed population of charge compensating cations. If the intracrystalline cation composition is mixed, sites in the vicinity of a cation will differ for each cation whether or not they occupy equivalent crystallographic positions. Further, in a mixed cation population the proportion of one cation to another may vary from one cavity to another so that the behavior of the cavities as multiple sorption sites may vary throughout the crystal (Barrer, 1978).

The presence of energetic heterogeneity of a system can be determined by plotting the isosteric heat of adsorption vs. the amount adsorbed. Energetic heterogeneity of the system will result in a decrease in the isosteric heat of adsorption as the amount sorbed increases. For small uptakes, the isosteric heat may decrease rather strongly with the amount adsorbed. This would be an indication that there are some local intracrystalline positions where the guest molecules are preferentially sorbed more exothermally than in the rest of the intracrystalline volume. At intermediate uptakes, the slope of this plot will usually decrease and become nearly constant.

The measurement of adsorption isotherms at different temperatures permits the calculation of the heat of adsorption as a function of surface coverage. When experimental data are reported as a set of adsorption isotherms for a particular gas-adsorbent system, the isosteric heat of adsorption is usually calculated (Bajusz and Goodwin, 1997). The isosteric heat of adsorption can be calculated from a series of isotherms by application of the Clausius-Clapeyron equation as follows

$$\Delta H_{ads} = R\left(\frac{d\ln P}{d(1/T)}\right)_n \tag{3}$$

Using the data from nitrogen and oxygen adsorption isotherms measured at 50°C, 25°C, and 0°C, the isosteric heats of adsorption were determined by evaluating the slope of a plot of ln (P) vs. $(1/T)$ at several coverages. The plots of ln (P_{N2}) vs. $(1/T)$ at several coverages for $Li_{94.5}Na_{1.5}$-X-1.0 (top) and $Li_{94.2}Na_{0.7}Ag_{1.1}$-X-1.0 (bottom) are shown in Figure 8. The isosteric heats of adsorption at different coverages were calculated for each of these materials and are shown in Figure 9. A similar analysis was also done for the oxygen and argon data, but these results are not shown. From the plots of the heats of nitrogen adsorption, shown in Figure 9, one

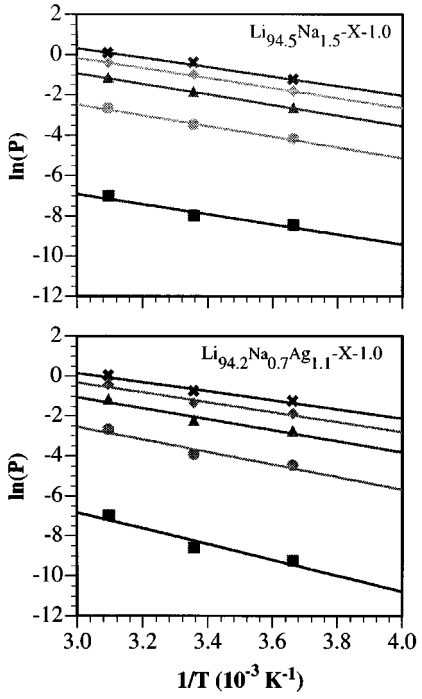

Figure 8. ln (*P*) vs. 1/T at different coverages for $Li_{94.5}Na_{1.5}$-X-1.0 (top) and $Li_{94.2}Na_{0.7}Ag_{1.1}$-X-1.0 (bottom).

can see that the isosteric heat of adsorption for N_2 on $Li_{94.2}Na_{0.7}Ag_{1.1}$-X-1.0 is quite high ($\approx$ 8 kcal/mol) at low coverages, but immediately drops sharply to become nearly horizontal. This indicates the presence of local intracrystalline sites where the N_2 is preferentially sorbed more strongly than at other sites within the intracrystalline volume. A comparison with the same plot of the isosteric heat of adsorption for N_2 for $Li_{94.5}Na_{1.5}$-X-1.0, which is essentially horizontal, shows that the energetic heterogeneity of the $Li_{94.2}Na_{0.7}Ag_{1.1}$-X-1.0 zeolite is due entirely to the incorporation of the approximately one Ag per unit cell. The plots of the heats of adsorption for O_2 and Ar were horizontal with coverage, indicating the interaction between the silver clusters and these guest molecules is much less than with the N_2. The approximate constant heat of adsorption with increasing coverage for the $Li_{94.5}Na_{1.5}$-X-1.0 is consistent with previously reported results (Bajusz and Goodwin, 1997), and likely indicates an energetically homogeneous surface.

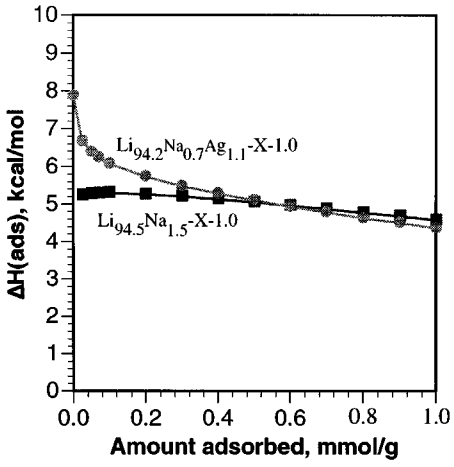

Figure 9. Isosteric heats of adsorption of N_2 for $Li_{94.5}Na_{1.5}$-X-1.0 and $Li_{94.2}Na_{0.7}Ag_{1.1}$-X-1.0.

Cation site location

For the X zeolites, the cation site designations are conventionally designated as SI (the center of the hexagonal prism), SI′ (opposite SI but located in the cubooctahedron), SII (single six-ring in the supercage), SII′ (opposite SII but inside the cubooctahedron), and SIII (near the four-ring windows in the supercage) (Breck, 1984).

Several studies have been employed in order to locate extra framework Li^+ cations in X, Y and A zeolites (Feuerstein and Lobo, 1998; Herden et al., 1982) using solid state NMR and neutron diffraction methods. It was found that the Li^+ ions fully occupy all 32 SI' sites and all 32 SII sites. The SIII sites were then occupied with the remaining Li^+ ions, 22 for Li_{86}-X-1.25, and 32 for Li_{96}-X-1.0. No occupancy of the SI sites was observed. Coe (1995) reported an occupancy "threshold" of 64 cations. Mixed Li_xNa_y-X zeolites which contained less Li^+ than this threshold amount did not show any increase in the N_2 adsorption capacity over that of the fully Na^+-exchanged materials. This indicated that only those Li^+ ions located in the SIII cation sites were interacting with the N_2 molecules. This result is interesting because, even though the SI and SI' sites are sterically inaccessible to the N_2 molecules, the SII sites are not; other cations, such as Ca^{2+}, do interact with N_2 when located in the SII positions.

Numerous studies have also been undertaken to identify the location of Ag^+ ions and Ag-clusters, typically by X-ray diffraction methods (Kim and Seff, 1978a,b; Gellens et al., 1981a,b) and far-infrared spectroscopy (Baker et al., 1985; Ozin et al., 1984). It was found that, for dehydrated, fully Ag^+-exchanged faujasite-type zeolites, the silver cations (or ground state atoms) were distributed among the six-ring sites (SI, SI', and SII for type X) and, for samples with high Al content, in the SIII locations. Gellens et al. (1981a) and Baker et al. (1985) showed the simultaneous occupancy of sites SI and SI' by linear (Ag^+-Ag^0-Ag^+) clusters. In general, all studies seemed to indicate that the Ag cations and atoms preferred the SI and SI' sites.

No studies have been conducted to identify the location of Li^+ and Ag^+ cations in mixed Li_xAg_y-zeolites. While it has been shown that the Ag^+ ions prefer the SI and SI' locations, it is known that the Li^+ ions also strongly prefer the SI' sites. Both of these sites are sterically inaccessible to the N_2 and O_2 molecules; so, the formation of silver clusters in these locations may not have a strong effect on the overall adsorptive characteristics of the mixed Li_xAg_y-X zeolites. Therefore, it is expected that the clusters, in these mixed cation zeolites, are instead formed at the N_2 and O_2 accessible SII and/or SIII locations due to competition with the Li^+ cations for the preferred SI and SI' locations. Logically, Ag-cluster formation at the SII sites would most enhance the adsorptive characteristics of mixed Li_xAg_y-X zeolites since these sites

have been shown to be noninteractive when occupied with Li^+ ions. Kim and Seff (1987) identified the location of Ag in mixed Na_xAg_y-A zeolites and found that the Ag ions prefer six-ring sites (such as the SI, SI', and SII in the X zeolites). This may indicate a preference for the SII sites in type X zeolites when the SI and SI' sites are unavailable (due to competition with Li^+).

Another possibility is that the Ag clusters were formed in the SI-SI' sites, and due to the strong field gradient that is generated by Ag^+, enhanced interactions with the N_2 molecules is still possible. This possibility would account for the fact that the optimal sorbent contained only, on average, approximately one Ag per unit cell, because each Ag_3^{2+} cluster was shared by three supercage cavities. Further work to identify the Ag cluster location(s) is in progress.

Nature of interaction

The total energy of physical adsorption ϕ_T is the result of the interactions between adsorbate molecules and interactions between the adsorbate molecules and the zeolite cavity wall (Razmuz and Hall, 1991). The ϕ_T is comprised of dispersive (D), repulsive (R), polarization (P), field-dipole (FD) interactions, field-quadrupole (FQ) interactions, and adsorbate energies. These can be written as follows

$$\phi_T = -(\phi_D - \phi_R) - \phi_P - \phi_{\mathrm{FD}} - \phi_{\mathrm{FQ}} - \phi_{\mathrm{AA}} \qquad (4)$$

The adsorbates of interest in this evaluation (N_2, O_2, and Ar) do not have permanent dipoles, and the coverages are low. Therefore, the field-dipole and adsorbate-adsorbate interactions can be ignored and Eq. 4 can be reduced to

$$\phi_T = -(\phi_D - \phi_R) - \phi_P - \phi_{\mathrm{FQ}} \qquad (5)$$

Because the N_2 and O_2 molecules are very similar in size and have comparable polarizabilities, the dispersive, repulsive, and polarization energies between the adsorbate and the extra framework cations are very similar. The quadrupole moment of the N_2 molecule is approximately four times that of the O_2 molecule and is primarily responsible for the difference in the adsorptive capacity for N_2 over that of O_2. Argon, which does not have a quadrupole moment, is more greatly affected by the polarization energies; for most zeolites, the Ar capacity is about the same as that of O_2.

The very high heat of binding of the N_2 molecules at very low pressures is probably due to very high electrostatic fields near the exposed charged Ag-clusters and their interaction with the quadrupole moment of the N_2 molecule. However, because there is also an increase in the adsorption of argon, which does not have a quadrupole moment, these charged clusters must also contribute to the total energy of physical adsorption by increased van der Waals and field-induced dipole energies and could possibly have a higher polarizing power than that of isolated silver cations.

Physical adsorption, however, is likely not the only contribution to N_2 adsorption in silver-containing zeolites. Yang et al. (1996), noting the high isosteric heat of adsorption for N_2 on Ag_{86}-X-1.25 zeolites combined with a relatively slow desorption of N_2 on the same, proposed some degree of weak π-complexation. The π-complexation character of the interaction was subsequently confirmed by *ab inito* molecular orbital calculations using N_2 and an Ag-X cluster model (Chen and Yang, 1996) and was referred to as ''weak chemisorption-assisted adsorption.''

PSA cycle description

A standard five-step PSA cycle that is presently used in industry for air separation (Leavitt, 1991) was used in this study. The steps involved in each cycle are as follows: (step I) pressurization with the feed gas, namely, 22% O_2 (mixture of O_2 and Ar) and 78% N_2; (step II) high-pressure adsorption with the feed gas, or feed step; (step III) cocurrent depressurization; (step IV) countercurrent blowdown; (step V) countercurrent low-pressure purge with the product of the feed step (oxygen).

All the above steps were of equal duration (30 s); thus, the time required for the completion of each PSA cycle was 2.5 min. The model assumed only two adsorbable components, O_2 and N_2. The oxygen component (22%) was actually a mixture of O_2 and Ar which have very similar adsorption isotherms for the sorbents of interest. The product of each cycle was comprised of a volumetric mixture of the output stream of the feed step and the cocurrent depressurization step. A portion of this product stream was used to purge the bed countercurrently in step V.

In order to compare the performance of the $Li_{94.5}Na_{1.5}$-X-1.0 and the $Li_{94.2}Na_{0.7}Ag_{1.1}$-X-1.0 sorbent developed in this work, the product throughputs of the two sorbents were studied under two different cycle conditions using computer simulations. In order to facilitate a fair comparison of the sorbent performance, the cycle conditions were optimized such that the product purity and product recovery obtained were the same for both the sorbents in each respective simulation run. In this work, the product purity, product recovery and product throughput are defined as follows

product purity

$$= \frac{(\text{amount of } O_2 \text{ from steps II and III})}{(\text{amount of } N_2 \text{ and } O_2 \text{ from steps II and III})} \qquad (6)$$

product recovery

$$= \frac{(O_2 \text{ from steps II and III}) - (O_2 \text{ used in step V})}{(O_2 \text{ fed in step I and step II})} \qquad (7)$$

product throughput

$$= \frac{[\text{amount of } O_2 \text{ produced per hour (kg/h)}]}{[\text{amount of adsorbent used in the bed (kg)}]} \qquad (8)$$

The mathematical model and the numerical method used for the PSA simulations in this study have been explained in detail in an earlier work (Rege and Yang, 1997). Hence, only the basic assumptions will be listed here. The model used assumes the flow of a gaseous mixture of two components in a fixed bed packed with spherical adsorbent particles. The bed is considered to be adiabatic and diffusional resistance is assumed to be negligible since the diffusion of O_2 and N_2 in the adsorbents is essentially instantaneous, as observed in this

Table 3. Parameters in the Temperature-Dependent Langmuir Isotherm of N_2 and O_2 for Adsorbents

Sorbent	Sorbate	k_1 (mmol/g)	k_2 (K)	k_3 (atm^{-1})	k_4 (K)	$-\Delta H$ (kcal/mol)
$Li_{94.5}Na_{1.5}$-X-1.0	O_2	1.14	239.2	2.20×10^{-3}	1,092	2.66
$Li_{94.5}Na_{1.5}$-X-1.0	N_2	1.69	134.4	1.19×10^{-3}	1,990	5.16
$Li_{94.2}Na_{0.7}Ag_{1.1}$-X-1.0	O_2	0.965	196.0	2.25×10^{-3}	1,212	3.00
$Li_{94.2}Na_{0.7}Ag_{1.1}$-X-1.0	N_2	2.12	64.82	7.78×10^{-3}	1,494	5.39

study. Thus, there is local equilibrium between the gas and the solid phase of each gas component. Axial dispersion for mass and heat transfer is assumed but dispersion in the radial direction is taken to be negligible. Axial pressure drop is neglected and ideal gas law is assumed to hold since pressures involved are near atmospheric. Also, the gas is assumed to have constant viscosity and heat capacity.

The pure component equilibrium amounts adsorbed on the respective adsorbents were fit using the well-known Langmuir isotherm with temperature-dependent terms. The equilibrium loading under mixture conditions were then predicted by the extended Langmuir equation in the simulation model

$$q_k^* = \frac{q_{m_k} b_k p_k}{1 + \sum_{j=1}^{m} b_j p_j} \qquad k = 1, 2 \tag{9}$$

The temperature dependence of the Langmuir parameters is assumed to be as follows

$$q_m = k_1 \exp(k_2/T) \qquad \text{and} \qquad b = k_3 \exp(k_4/T) \tag{10}$$

The values of the Langmuir equation terms for $Li_{94.5}Na_{1.5}$-X-1.0 and $Li_{94.2}Na_{0.7}Ag_{1.1}$-X-1.0 sorbents, as well as the heats of adsorption are given in Table 3.

Table 4. Adsorption Bed Characteristics and Operating Conditions for PSA Simulations

Bed length	2.5 m
Diameter of adsorber bed	1.0 m
Bed external porosity	0.40
Bed density	720 kg/m^3
Heat capacity of gases	6.87 cal/mol/K
Heat capacity of bed	0.28 cal/g/K
Wall temperature	298 K (ambient)
Feed gas composition	78% N_2, 22% O_2
Feed gas temperature	298 K
Axial dispersion coefficient (D_{ax})	5×10^{-3} m^2/s

Simulation results

The PSA bed characteristics and the operating conditions used are summarized in Table 4. The PSA cycle parameters were chosen as close to industrially acceptable values as possible. The pressure ratio, which is the ratio of the feed pressure (P_H) to the desorption pressure (P_L), is an important operating characteristic, and it has been shown that a value of 3 suffices for an optimal PSA performance using the Li-X-1.0 sorbent (Rege and Yang, 1997). The same pressure ratio was employed for the comparison of the $Li_{94.5}Na_{1.5}$-X-1.0 and $Li_{94.2}Na_{0.7}Ag_{1.1}$-X-1.0 sorbents in this work. As can been seen from Table 5, run 1 comprises a feed pressure of 1.0 atm, while run 2 was carried out at a higher feed pressure of 1.2 atm. The cocurrent depressurization pressure, feed velocity, and purge velocity were optimized so as to obtain the same product purity and recovery for both the sorbents. As seen from the O_2 and N_2 isotherms in Figure 10, the $Li_{94.2}Na_{0.7}Ag_{1.1}$-X-1.0 sorbent has a higher capacity for N_2. From the extended Langmuir isotherm (Eq. 9), it follows that the higher N_2 loading further suppresses the O_2 loading under mixture conditions and, as a result, the working capacity of the $Li_{94.2}Na_{0.7}Ag_{1.1}$-X-1.0 sorbent further increases. Hence, the amount of bed utilization (or the depth of propagation of the N_2 wavefront in the bed) of the $Li_{94.2}Na_{0.7}Ag_{1.1}$-X-1.0 sorbent was lower than that of the $Li_{94.5}Na_{1.5}$-X-1.0 sorbent under identical cycle conditions. The higher capacity of the $Li_{94.2}Na_{0.7}Ag_{1.1}$-X-1.0 sorbent could be exploited by employing higher feed throughputs and lower cocurrent depressurization pressure without significantly lowering product purity and recovery. An obvious outcome of the high capacity of the $Li_{94.2}Na_{0.7}Ag_{1.1}$-X-1.0 sorbent was a higher product throughput compared to that of the $Li_{94.5}Na_{1.5}$-X-1.0 sorbent when the other performance parameters (that is, product purity and recovery) were kept the same. However, the heats of adsorption of the two com-

Table 5. PSA Simulation Operating Conditions and Results

Sorbent	P_H (atm)	P_L (atm)	P_{CD} (atm)	U_H (m/s)	U_L (m/s)	O_2 Product Purity (%)	O_2 Product Recovery (%)	Product Throughput (kg O_2/h/kg Ad.)
Run 1								
$Li_{94.5}Na_{1.5}$-X-1.0	1.0	0.33	0.70	0.48	0.38	96.11	62.03	4.84×10^{-2}
$Li_{94.2}Na_{0.7}Ag_{1.1}$-X-1.0	1.0	0.33	0.69	0.60	0.42	96.42	62.74	5.40×10^{-2}
Run 2								
$Li_{94.5}Na_{1.5}$-X-1.0	1.2	0.4	0.70	0.40	0.38	90.68	78.02	6.31×10^{-2}
$Li_{94.2}Na_{0.7}Ag_{1.1}$-X-1.0	1.2	0.4	0.71	0.50	0.38	90.83	78.48	7.01×10^{-2}

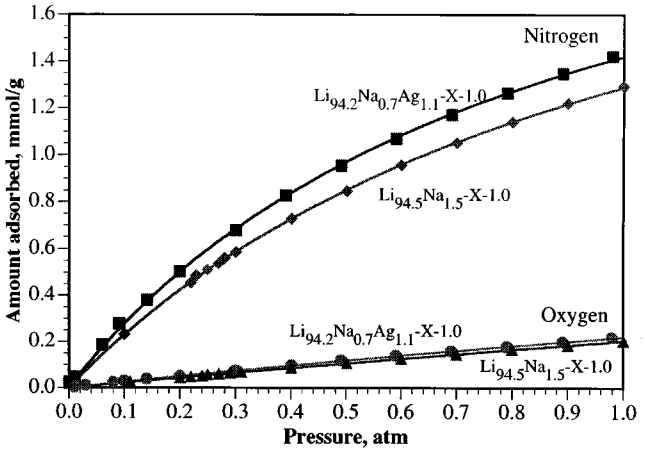

Figure 10. N_2 and O_2 isotherms for $Li_{94.2}Na_{0.7}Ag_{1.1}$-X-1.0 dehydrated *in vacuo* at 450°C and for $Li_{94.5}Na_{1.5}$-X-1.0 dehydrated *in vacuo* at 350°C.

All isotherms were measured at 25°C.

ponents on the $Li_{94.2}Na_{0.7}Ag_{1.1}$-X-1.0 sorbent were also higher than those on the $Li_{94.5}Na_{1.5}$-X-1.0 sorbent. Severe temperature excursions in adsorption-desorption cycles are known to adversely affect PSA separation performance (Yang, 1997a), this is true to some degree even for air separation where the adverse effects are not strong but significant (Rege and Yang, 1997). Fast cycling will decrease the effects. A PSA simulation run is necessary to critically evaluate the importance of higher N_2 loading and higher heat of adsorption in case of $Li_{94.2}Na_{0.7}Ag_{1.1}$-X-1.0 sorbent and the accompanying heat effects.

The results of the simulation runs are shown in Table 3. It can be seen from run 1 (feed pressure: 1 atm) that the O_2 product throughput obtained by using $Li_{94.2}Na_{0.7}Ag_{1.1}$-X-1.0 sorbent was 5.4×10^{-2} kg O_2/h/kg-sorbent compared to the throughput of 4.8×10^{-2} kg O_2/h/kg-sorbent offered by $Li_{94.5}Na_{1.5}$-X-1.0 sorbent. The corresponding O_2 product purity and recovery were approximately 96% and 62%, respectively. There is an improvement of 12.5% in the product throughput which translates into considerable savings in capital and operating costs since a higher product throughput implies a smaller bed requirement for the same desired production. Another run was done at a different feed pressure of 1.2 atm with the cycle conditions optimized to produce O_2 product at 90.7% purity and 78% recovery. In this case as well, the product throughput of the $Li_{94.2}Na_{0.7}Ag_{1.1}$-X-1.0 sorbent was found to be higher (7×10^{-2} kg O_2/h/kg sorbent), compared to that of the $Li_{94.5}Na_{1.5}$-X-1.0 sorbent (6.3×10^{-2} kg O_2/h/kg sorbent). Thus, the product throughput of the $Li_{94.2}Na_{0.7}Ag_{1.1}$-X-1.0 sorbent is higher by 11% even at a lower O_2 product purity requirement. The values of the throughputs obtained in this study were found to have an order of magnitude agreement with those published for Li-X-1.0 sorbent in literature (Leavitt, 1991). From the simulated bed profiles, it was observed that temperature deviations from the feed temperature of 25°C due to the adsorption heat effects were about 17°C for the $Li_{94.2}Na_{0.7}Ag_{1.1}$-X-1.0 sorbent, while it was only 12°C for the $Li_{94.5}Na_{1.5}$-X-1.0 sorbent. However, from the results, it appears that the advantage of higher N_2 loading on the $Li_{94.2}Na_{0.7}Ag_{1.1}$-X-1.0 more than compensates the lowering of PSA performance due to higher heat effects. Hence, it is evident from the previous two examples that the $Li_{94.2}Na_{0.7}Ag_{1.1}$-X-1.0 sorbent is superior to the $Li_{94.5}Na_{1.5}$-X-1.0 sorbent for air separation by PSA.

Acknowledgment

Neutron Activation Analyses (NAA) were conducted in the Ford Nuclear Reactor of the Phoenix Memorial Laboratory at the University of Michigan. The analyses were coordinated by Leah Minc of the Michigan Memorial Phoenix Project.

Notation

b = Langmuir parameter, atm^{-1}
D_{ax} = axial dispersion coefficient in adsorbent particles, m^2/s
ΔH = heat of adsorption, kcal/mol
k_1 = Langmuir temperature dependence constant, mmol/g
k_2, k_4 = Langmuir temperature dependence constant, K
k_3 = Langmuir temperature dependence constant, atm^{-1}
p = partial pressure, atm
P = total pressure, atm
q_m = Langmuir parameter, mmol/g/atm
q^* = equilibrium adsorbate loading, mmol/g
T = temperature, K
U = interstitial gas velocity, m/s

Subscripts

CD = Intermediate pressure corresponding to the cocurrent depressurization step
i = species i
j, k = gas-phase component index
L = low-pressure corresponding to purge step

Literature Cited

Bajusz, I. G., and J. G. Goodwin, "N_2 Adsorption in LiX Zeolite: Isotopic Transient Analysis," *Langmuir*, **13**, 6550 (1997).
Baker, M. D., G. A. Ozin, and J. Godber, "Far-Infrared Studies of Silver Atoms, Silver Ions, and Silver Clusters in Zeolites A and Y," *J. Phys. Chem.*, **89**, 305 (1985).
Barrer, R. M., *Zeolites and Clay Minerals as Sorbents and Molecular Sieves*, Academic Press, London (1978).
Breck, D. W., *Zeolite Molecular Sieves*, R. E. Krieger Publishing, Malabar, FL (1984).
Chao, C. C., "Process for Separating Nitrogen from Mixtures Thereof with Less Polar Substances," U.S. Patent No. 4,859,217 (1989).
Chao, C. C., J. D. Sherman, J. T. Mullhaupt, and C. M. Bolinger, "Mixed Ion-Exchanged Zeolites and Processes for the Use Thereof in Gas Separation," U.S. Patent 5,174,979 (1992).
Chen, N., and R. T. Yang, "An *ab Initio* Molecular Orbital Study of Adsorption of Oxygen, Nitrogen and Ethylene on Silver-Zeolite and Silver Halides," *Ind. Eng. Chem. Res.*, **35**, 4020 (1996).
Coe, C. G., J. F. Kirner, R. Pierantozzi, and T. R. White, "Nitrogen Adsorption with a Ca and/or Sr Exchanged Zeolite," U.S. Patent No. 5,152,813 (1992).
Coe, C. G., *Access in Nanoporous Materials*, T. J. Pinnavaia and M. F. Thorpe, eds., Plenum Press, New York, p. 213 (1995).
Feuerstein, M., and R. F. Lobo, "Characterization of Li Cations in Zeolite LiX by Solid-State NMR Spectroscopy and Neutron Diffraction," *Chem. Mater.*, **10**, 2197 (1998).
Fitch, F. R., M. Bulow, and A. F. Ojo, "Adsorptive Separation of Nitrogen and Other Gases," U.S. Patent No. 5,464,467 (1995).
Gellens, L. R., W. J. Mortier, and J. B. Uytterhoeven, "On the Nature of the Charged Silver Clusters in Zeolites of Type A, X and Y," *Zeolites*, **1**, 11 (1981a).
Gellens, L. R., W. J. Mortier, R. A. Schoonheydt, and J. B. Uytterhoeven, "The Nature of the Charged Silver Clusters in Dehy-

drated Zeolites of Type A,'' *J. Phys. Chem.*, **85**, 2783 (1981b).
Gellens, L. R., J. V. Smith, and J. J. Pluth, ''Crystal Structure of Vacuum-Dehydrated Silver Hydrogen Zeolite A,'' *J. Amer. Chem. Soc.*, **105**, 51 (1983).
Habgood, H. W., ''Adsorptive and Gas Chromatographic Properties of Various Cationic Forms of Zeolite X,'' *Can. J. Chem.*, **42**, 2340 (1964).
Herden, H., W. D. Einicke, R. Schollner, W. J. Mortier, L. R. Gellens, and J. B. Uytterhoeven, ''Location of Li-ions in Synthetic Zeolites X and Y,'' *Zeolites*, **2**, 131 (1982).
Huang, Y., ''Adsorption in AgX and AgY Zeolites by Carbon Monoxide and Other Simple Molecules,'' *J. Catalysis*, **32**, 482 (1974).
Jacobs, P. A., J. B. Uytterhoeven, and H. K. Beyer, ''Some Unusual Properties of Activated and Reduced AgNaA Zeolites,'' *J. Chem. Soc. Faraday Trans. 1*, **75**, 56 (1979).
Kim, Y., and Seff, K., ''The Octahedral Hexasilver Molecule. Seven Crystal Structures of Variously Vacuum-Dehydrated Fully Ag^+-Exchanged Zeolite A,'' *J. Amer. Chem. Soc.*, **100**, 6989 (1978a).
Kim, Y., and K. Seff, ''The Hexasilver Molecule Stabilized by Coordination to Six Silver Ions. The Structure of $(Ag^+)_6(Ag_6)$. The Crystal Structure of an Ethylene Sorption Complex of Partially Decomposed Fully Ag^+-Exchanged Zeolite A,'' *J. Amer. Chem. Soc.*, **100**, 175 (1978b).
Kim, Y., and K. Seff, ''Crystal Structure of Fully Dehydrated, Partially Ag^+-Exchanged Zeolite 4A, $Ag_{7.6}Na_{4.4}$-A. Ag^+ Ions Prefer 6-Ring Sites. One Ag^+ Ion is Reduced,'' *J. Phys. Chem.*, **91**, 671 (1987).
Knaebel, K. S., and A. Kandybin, ''Pressure Swing Adsorption System to Purify Oxygen,'' U.S. Patent 5,226,933 (1993).
Kuhl, G. H., ''Crystallization of Low-Silica Faujasite ($SiO_2/Al_2O_3 \approx$ 2.0),'' *Zeolites*, **7**, 451 (1987).
Leavitt, F. W., ''Air Separation Pressure Swing Adsorption Process,'' U.S. Patent No. 5,074,892 (1991).
McKee, D. W., ''Separation of an Oxygen-Nitrogen Mixture,'' U.S. Patent No. 3,140,933 (1964).
Ozin, G. A., M. D. Baker, and J. Godber, ''Direct Observation of the Reversible Redox Couple $Ag_3^{2+} \Leftrightarrow Ag_3^0$ in Silver Zeolite A by Fourier Transform Far-Infrared Spectroscopy,'' *J. Phys. Chem.*, **88**, 4902 (1984).
Razmuz, D. M., and C. K. Hall, ''Prediction of Gas Adsorption in 5A Zeolites Using Monte Carlo Simulation,'' *AIChE J.*, **37**, 769 (1991).
Rege, S. U., and R. T. Yang, ''Limits for Air Separation by Adsorption with LiX Zeolite,'' *Ind. Eng. Chem. Res.*, **36**, 5358 (1997).
Yang, R. T., *Gas Separation by Adsorption Processes*, Butterworth, Boston (1987) (Reprinted by Imperial College Press, London and World Scientific Publishing Co., River Edge, NJ (1997a).
Yang, R. T., ''Recent Advances and New Horizons in Gas Adsorption—with a Focus on New Sorbents,'' *Preprints Topical Conf. Separ. Sci. Tech.*, W. S. W. Ho and R. G. Luo, eds., AIChE, New York, p. 14 (1997b).
Yang, R. T., Y. D. Chen, J. D. Peck, and N. Chen, ''Zeolites Containing Mixed Cations for Air Separation by Weak Chemisorption-Assisted Adsorption,'' *Ind. Eng. Chem. Res.*, **35**, 3093 (1996).
Yang, R. T., and N. D. Hutson, ''Lithium-based Zeolites Containing Silver and Copper and Use Thereof for Selective Adsorption,'' U.S. patent pending, Serial Number 60/114371 (filed Dec. 30, 1998).

Manuscript received Sept. 28, 1998, and revision received Jan. 28, 1999.

Correction

In the article titled ''Concentration Profile for Linear Driving Force Model for Diffusion in a Particle'' (January 1999, p. 196), the two sentences preceding Eq. 9, ''$A(t)$ and $B(t)$ can be solved from the two boundary conditions ...'' should be replaced by the following:

For $A(t)$ and $B(t)$, $B(t)$ is first solved such that Eq. 8 leads directly to Glueckauf's LDF expression for all values of n ($n \geq 2$). A general expression for $A(t)$ is given by Eq. 9. The solution for $A(t)$ must satisfy the requirement that the transient volume-average uptake, $\bar{q}_i(t)$, calculated from the concentration profile is always equal to that calculated directly from the LDF expression. As shown below, Eq. 9 satisfies this requirement only when $n = 2$ and 5. Moreover, an additional requirement for $A(t)$ is that the negative portion of the concentration profile near $r = 0$ at short times is minimized.